POSSIBILITIES OF OBSERVING AIR POLLUTION FROM ORBITAL ALTITUDES

By Dr. A. Barringer
President, Barringer Research Corporation
Ontario, Canada

Abstract

Research carried out over a number of years has indicated the feasibility of monitoring global air pollution from orbiting satellites. Data on the worldwide buildup of pollution levels on a regional scale is at present very meager. It has been established that carbon dioxide is gradually accumulating in the atmosphere and the long term possible climatic effects are some cause for concern. Far less is known about the buildup of other gases and of aerosols, and satellites could provide a most useful platform for studying trends and providing warnings of any general deterioration of the atmospheric environment.

Optical methods show considerable promise of measuring the burdens of pollution, both gaseous and particulates. Important pollution gases, such as sulfur dioxide, nitrogen dioxide, carbon monoxide, and ozone, as well as some hydrocarbon vapors, appear amenable to optical remote sensing. Satellite platforms for carrying out this work would not compete with ground monitoring stations but rather supplement them with a different type of data which could be integrated with ground level measurements to provide an all-embracing picture of pollution buildup, mass migration, and dissipation.

Acknowledgments

The author acknowledges the support received from many agencies contributive to the development of correlation spectroscopy and interferometry including NASA, MAS, MSFC, HQ, EPA, DEMR, DRB, NRC Ottawa, USAF and U.S. Army, and finally NASA-LRC and General Electric for the COPE interferometer.

Introduction

A growing awareness of the earth's finite capability to divest itself of the increasingly large tonnages of atmospheric pollutants, results from man's activities, has placed increased emphasis on the need for continuous monitoring of airborne contaminants on a regional and global scale.

The enormous expansion in the use of fossil fuels by the industrialized nations of the world has not only created serious problems of air quality around the centers of population, but the impact of mass transport of toxic contaminants to hitherto unspoiled regions of the world is becoming increasingly apparent. For example, in Scandinavia it is claimed that sulfur dioxide from Great Britain is contributing to the steadily increasing acidity of lakes in that region and to the decrease in lichen growth on the mountains of Norway. With the advent of remote sensing measurements from satellites or aircraft, it will be possible for the first time to establish the amount of mass transfer of sulfur dioxide across the North Sea and eliminate conjecture on this point.

Satellite and aircraft monitoring of atmospheric contaminants using remote sensors adds a new dimension to existing methods of pollution measurement. Downward-looking satellite systems will provide a measure of the total burden of specific contaminants in the earth's atmosphere and will permit considerable extension and extrapolation of ground-based data. Whereas the satellite monitor will provide global maps of pollutant distribution, it cannot alone provide absolute concentrations. On the other hand, it is simply not feasible to cover the whole earth with a comprehensive network of ground stations. Therefore, satellite monitoring will be complementary to and not competitive with ground monitoring methods.

In addition to enabling the scientist to study the circulation patterns of large air masses in the global atmosphere, the satellite sensor will aid in the investigation of interacting effects of pollution, the effective lifetimes of specific gaseous species in the atmosphere, and the long term effects of a sustained buildup of polluting materials.

Carbon monoxide, for example, is being added to the atmosphere at a rate which would cause the global background to almost double every 2 years if we take into account the various removal mechanisms or sinks now known to exist. Since this is not happening and, in fact, the available data, albeit very meager, show no apparent increase in the mean global concentration in the last 20 years, it is clear that carbon monoxide is being removed from the atmosphere by one or more mechanisms not yet fully understood.

The global mapping of carbon monoxide from a satellite offers the intriguing possibility of being able to correlate the distribution of carbon monoxide over the global surface, with geographical features and circulating air masses, in such a way as to delineate the carbon monoxide sink anomalies. It may also be possible to investigate possible modes of carbon monoxide dissipation in the upper atmosphere by orienting the satellite sensor to observe the earth's limb using the direct radiation of the sun.

There is also serious concern that the slow but relatively steady buildup of carbon dioxide (0.66 ppm per month) could have a long term warming effect on the earth's climate. Projections of this so-called greenhouse effect are complicated by the increasing burden of particulate or aerosol pollution, which could conceivably produce an effect in the opposite sense; i.e., a cooling trend in the global climate.

A relatively recent development, posing possible threats to the global ecology, is the advent of the supersonic aircraft and large rocket engines which are capable of dumping large tonnages of spent pollutants and water vapor in the upper atmosphere, where the photochemical activity is very high and the meteorological conditions of dispersion are entirely different from those prevailing in the troposphere.

With satellite remote sensing equipment of appropriate design it should be possible to monitor the behavior of these high altitude pollutants more effectively than from aircraft or ground-based observations.

Monitoring From Orbital Altitudes

Remote sensing of atmospheric material requires a source of radiant energy, and for nadir-looking sensors, two forms of solar radiation may be received (Fig. 1). One is reflected solar radiation which bounces off the surface of the earth or its atmosphere and covers the spectral region between 3000 Å in the ultraviolet and about 4 μm in the near infrared. The other is thermal radiation emitted from the earth as a blackbody at 300° K which lies in the region between about 4 and 15 μm. Sulfur dioxide exhibits strong absorption spectra in the 3000 to 3200 Å region, and nitrogen dioxide shows almost continuous but very irregular absorption features from the ultraviolet to the visible region. The infrared regions are particularly rich in absorption and emission spectra, and in fact, virtually all gaseous pollutants of interest report in the 1 to 15 μm region. The physics of the measurements of atmospheric gases is relatively straightforward in the cases of those species which absorb in the ultraviolet, visible, or near infrared but increases in complexity for those gases which exhibit absorption in the thermal regions of the infrared. In the latter case the temperature of the gas being measured becomes critical, and when high altitude measurements are being made, the effects of pressure also have to be taken into consideration. Also, in both the near and thermal infrared the region is so heavily populated with gas spectra, many of which tend to overlap, that the achievement of adequate sensor sensitivity with good interference rejection is a problem of some magnitude.

In the ultraviolet and visible regions the interference problem is much less severe; however, the spectral signatures of near-surface gases are significantly weakened by atmospheric absorption and backscatter. The resulting signal is particularly troublesome in the ultraviolet. These effects are shown diagrammatically in Figure 2.

It is possible to measure concentrations of a gas by noting the absorption obtained at one wavelength corresponding to a strong absorption band in the gas, and comparing it with the absorption at an adjacent wavelength where the gas does not absorb. This simple technique, however, tends to be subject to interferences because of the fact that absorption bands are seldom unique, and it is generally impossible to pick a pair of wavelengths which will not suffer from some differential absorption because of the presence of gases other than the one being sought.

An effective method of combating this interference problem is to correlate a substantial portion of the absorption spectrum of the gas being measured against a stored replica or mask of the spectrum. The term "correlation spectroscopy" has been coined to describe this technique. A significant number of prototype instruments have been

constructed employing this principle. Over the past 5 years, various configurations of the correlation spectrometer have been extensively evaluated. In September 1969 a high altitude balloon experiment was performed to test the feasibility of monitoring atmospheric sulfur dioxide and nitrogen dioxide from above the ozonosphere.

While correlation spectroscopy is convenient to apply in the ultraviolet, visible, and near-infrared portions of the spectrum, it becomes more convenient to use interferometric methods in the middle and far infrared. Detectors are far less sensitive in this region and there is a much greater requirement for large light throughput in the detection device. This condition is satisfied by an interferometer, and by scanning the path difference in the interferometer, an interferogram can be generated which may be converted into a spectrum by means of a Fourier transform operation in a computer. In the correlation interferometer, however, the gas correlation is carried out directly in the interferometer against a stored replica of the interferogram of the gas being detected. The intermediate Fourier transform step is omitted, thereby greatly simplifying the approach. This is possible because of the fact that the Fourier transform of a gas spectrum is as unique as is the spectrum itself.

Remote Sensing in the Ultraviolet and Visible

A remote sensing correlation spectrometer for SO_2, NO_2, and I_2 was developed and extensively evaluated in various airborne measurement programs. The results of these tests were so encouraging that a high altitude balloon experiment was conceived as a means of testing the feasibility of monitoring SO_2 and NO_2 concentrations in the lower atmosphere from satellite altitudes; i.e., from above the ozonosphere.

Thus, a high altitude balloon project was sponsored jointly by the NASA Manned Spacecraft Center (MSC) and the Canadian Department of Energy Mines and Resources. Chicago was selected as the ideal site because of its large population, heavy industrial activity, excellent ground-monitoring network, and its proximity to Lake Michigan as a large background area. The prime aim of this experiment was to see how large the SO_2 and NO_2 signals would be when viewed from high altitude, normally 114 000 ft. At this altitude the balloon would be above most of the ozonosphere, which is the upper atmospheric layer of ozone which acts as a powerful absorber of ultraviolet light. When using the balloon platform the signals of the polluting gases are impressed upon the reflected light from the earth's surface, the light having made two passes through the air layer. Therefore, apart from its normal alternation, the signal is diluted by atmospheric scattering.

For the balloon flight, two correlation spectrometers were flown, one measuring SO_2 in the ultraviolet region; the other measuring NO_2 in the blue visible. These two gases had two critical problems in common, Fraunhofer line interference in the solar spectrum and dilution of their spectral signatures because of atmospheric absorption and scattering. Sulfur dioxide measurements had the added disadvantage, caused by the strong absorption of the ultraviolet radiation by the ozonosphere and the greater scattering of the shorter wavelengths compared to that which takes place in the visible region where the NO_2 was measured. Mathematical models had been developed and computer programs had been generated to model the instrument's performance to a variety of outside interferences and to calculate the optimum mask designs for balloon spectrometers.

Thus, it was that early in September 1969 when two spectrometers were flown over Chicago at 114 000 ft. Their field of view was approximately 1 deg by 1 deg which resulted in ground resolution patch of 0.5 square mile. Because of polarization effects, the entire gondola was stabilized to prevent azimuthal rotation and thereby keep constant sun angle. This was achieved through the use of a solar tracker device.

Also incorporated was a flip mirror to alter the viewing direction of the spectrometer from a ground vertical to a 24 deg angle away from the solar side so that two tracks of data were generated for SO_2 and NO_2, respectively. The chart records generated during the flight were returned to Toronto for digitization, and the data were then reduced by a computer and plotted in various map presentations. Intermittent cloud coverage beneath the float path of the balloon caused voids in the data. Simultaneous with the balloon flight, we obtained vertical profiles from the correlation spectrometer mounted in a station wagon which traversed the same float path as the balloon as far as was possible. Also the noontime values of SO_2 were obtained from the automatic city-wide air monitoring network in Chicago which

measured ground level concentrations. All of these data were assessed, reduced, and plotted on a digitized map of the Chicago area.

Figure 3 shows the computerized plot of the SO_2 spectrometer output signals. The spectrometer's output readings are shown plotted as discrete values on a baseline, which is the ground tract of the sensor's field of view when the flip mirror was in the 24 deg position. The circular but fortuitous float path of the balloon was the result of unstable wind vectors at float altitude, which is characteristic of upper level winds in late summer. The measurements are shown as discrete values rather than as a continuous analog signal because of the continuous grating scan system employed in the sensor.

Figure 4 shows similar data obtained when the viewing direction was vertically downward. The NO_2 data and the 24 deg case are shown in Figure 5 and in Figure 6 for the ground vertical case.

Note that in Figures 3 and 6 that, apart from voids in the data resulting from calibration intervals and intermittent cloud cover as previously mentioned, there is very substantial agreement between the balloon data and the concentrated sources of pollution in the Chicago metropolitan area.

Figure 1 shows the manually plotted three-dimensional profile of the station wagon data. The primary objective of the station wagon traverse was to obtain, as closely as possible, time and space coincident measurements of vertical burden SO_2 along the balloon ground track. Because of the unexpected departure of the balloon from the planned east-to-west trajectory, comparative measurements were possible only at the intersection of the station wagon and the balloon ground track near the Chicago monitoring station no. 23 (Fig. 7). The upward looking measurement was some 29 times larger than the downward-looking balloon measurement, indicating a dilution factor of 29 [1].

The value is some 2 to 3 times smaller than theoretical estimates but in view of the uncertainties involved, it is quite encouraging and represents an interesting first attempt at dilution measurements through the global atmosphere.

The results obtained during the balloon flight prove conclusively the viability of the correlation technique to monitor SO_2 in the ultraviolet spectral region and NO_2 in the blue visible by clearly demonstrating that solar reflected radiation, modified by target gas signatures impressed at the earth's surface, can be obtained at satellite altitudes. Also, it should be added, the characteristics of the signals obtained at the balloon were identical to those theoretically produced by mathematical modeling.

Remote Sensing With Ground Chopper

As indicated earlier, whereas attenuation and scattering are most severe in the short wavelength regions of the spectrum, other problems become paramount in the infrared. In the latter case these include the thermal structure of the atmosphere, temperature and emissivity of the target gases, and temperature and emissivity of the earth's surface. The concept of the ground chopper was formulated to combat these problems. This concept is based on the assumption that the atmosphere is a homogeneous scatterer or at least only a slowly changing scatterer, thus a spatial scan through the atmosphere should give, at the most, only a slowly varying signal because of scattered radiation. Conversely, ground reflectivity changes within the instantaneous field of view of an instrument will cause a rapid modulation of that radiation which has passed completely through the atmosphere down to the ground and back to the sensor. A frequency filtering separation can then be performed to separate the low frequency ground reflection components. Furthermore, a frequency analysis of the data gives information about the spatial terrain characteristics which cause changes in the incident power, and the amplitude frequency spectrum may be written as a Fourier transform of the time-varying current in the detector.

Based upon the successful completion of mathematical modeling and system studies, an instrument design was developed and an instrument constructed. The ground chopper instrument comprised a two-channel radiometer. One channel was set to monitor strongly scattered spectral energy in the wavelength region of 3100 Å, while the other channel was set to monitor the 4400 Å component where the scattering is much less severe. The 3100 Å region corresponds to the SO_2 absorption spectrum, while the 4400 Å corresponds to that of NO_2 absorption. The radiometer was equipped with a telescope and means of decreasing the field of view which thereby decreased the ground coverage resolution. The instrument was equipped with electronics to process the outputs of the phototube detectors, and provide automatic gain control to these tubes.

The ground chopper instrument that was constructed is shown in Figure 8, which shows the optical arrangement of the instrument. The wavelengths were selected by interference filters which were located at the face of the photomultiplier tubes to reduce scattered light contaminations. The instrument was flown at Yellowknife, Northwest Territory.

Our results show that even for this comparatively clean northern atmosphere the amount of scattered light received at approximately 1.5 km altitude was about 2 to 3 times greater than the directly reflected component in the 3100 A region; the amount of scattering received at 4400 Å was, of course, significantly less. The amount of ground chopping was found to be as high as 25 percent at an altitude of 150 m above the terrain surface when the field of view was reduced to a few feet on the ground. When the field of view was increased to approximately 20 ft on the ground, approximately 8 percent modulation was obtained. Frequency analysis of the ground chopper signal was performed and showed that, over the city of Yellowknife, the overall chopped signal amplitude tended to increase while the higher frequency constant decreased. It can be assumed that this is because of the nature of the terrain in Yellowknife, and that this situation would probably change for other locations (Figs. 9 through 11). The ground chopper experiment has indicated that while providing adequate high resolution employed in the foreoptics of the downward-looking telescope, a significant portion of the signal reflected from the ground surface is modulated by spatial changes in the ground albedo. Since it is a fact that the reflectance spectra of terrain materials are relatively flat in the ultraviolet, it is possible to assume that the modulated components of light at two closely adjacent wavelengths in the ultraviolet will be of identical intensity, providing that there are no gases present in the atmosphere which differentially absorb these two wavelengths. Conversely, the differential intensity of the ac components of two closely adjacent ultraviolet wavelengths, which have been reflected from the ground and modulated by fluctuations in ground albedo, can be used to measure the presence of an atmospheric gas which has a differential absorption at the two wavelengths. This is a simplified example which illustrates the aim of the ground chopper technique. In practice, the two adjacent wavelengths employed are sets of wavelengths which correspond to the sets used in the correlation techniques which have been described.

It will be appreciated that the method is, in a sense, inefficient in that it discards a considerable proportion of the light reflected from the ground. However, it has the advantage of automatically eliminating the atmospheric scattered component, which cannot be adequately eliminated by mathematical modeling techniques.

Although the method is most applicable in the ultraviolet for sulfur dioxide monitoring, it is also feasible to use it for nitrogen dioxide monitoring in the blue portion of the visible spectrum. Terrain reflectance curves are still relatively flat in this area, making the errors caused by spectral gradients small.

Therefore, the ground chopping technique appears to offer an opportunity for measuring the total burden of gas between an aircraft or spacecraft and the ground without interference caused by scattering effects in the atmosphere.

Remote Sensing in the Infrared

Whereas atmospheric scattering and attenuation are of major importance in the ultraviolet and visible, at increasing wavelengths the ability to penetrate haze and smoke improves markedly. Over certain wavelength bands in the infrared, however, the natural atmospheric constituents — water vapor, CO_2, and ozone — absorb heavily, creating, to all intents and purposes, opaque regions of the spectrum (Fig. 12). Between 1 and 15 μm, roughly 50 percent of the spectrum is unusable for satellite monitoring purposes. In the remaining regions, i.e., the atmospheric windows, these materials absorb only weakly, and it is the task of the sensor design to select an atmospheric window in which the target gas has sufficiently intense spectral signature for monitoring from orbital altitudes. The most useful atmospheric windows are, approximately:

0.95 - 1.1 μm

1.2 - 1.35 μm

1.5 - 1.8 μm

2.0 - 2.5 μm

3.3 - 4.1 μm

4.5 - 5.0 μm

8.0 - 13.0 μm

Absorption spectra of several of the most important atmospheric pollutants are shown in Figure 13.

Figures 14 and 15 show, in somewhat higher resolution, spectra of six hydrocarbons which together represent almost 60 percent of the total hydrocarbon emissions of the automobile. Also ethylene, propylene, and 1, 3 butadiene (Fig. 14) constitute 46 percent of the photochemical reactivity of auto exhaust [2]. A comparison of these components with the relatively nonreactive methane, acetylene, and ethane suggests a potential for selective remote sensing of these gaseous components in polluted atmospheres, which constitute the principal smog-forming potential of photochemical smogs over urban areas.

In high resolution, many of the gases of interest exhibit fine spectral detail, which is unique to that molecular species. A good example of this is the first overtone of CO which is shown in Figures 12 and 13 at 2.3 μm in low resolution and in Figure 16 in high resolution.

This type of fine detail may be employed to separate a gas from strong interferents, as is being done for CO in the Barringer correlation interferometer used in the NASA/General Electric Carbon Monoxide Pollution Experiment (COPE) program mentioned earlier.

The choosing of a spectral region for the COPE experiment also illustrates two types of problems which occur in the infrared region.

The two strongest bands for the CO infrared spectrum are the 1-0 fundamental at 4.6 μm and the 2-0 harmonic at 2.3 μm. The 4.6 band, which is about 100 times stronger, is in the thermal region and is relatively clear of interferents, while the weaker overtone is overlapped by interferents but is in what may be called the transmission region. That is, when we consider the radiative transfer equation for the satellite observing geometry of Figure 17, namely,

$$I(\mu) = \left[I_o \exp - \int_0^{Z_1} \alpha \, ds'' + \int_0^{Z_1} \beta \exp - \int_{s'}^{Z_1} \alpha \, ds'' \, ds' \right] \rho$$

$$\times \exp - \int_{Z_1}^{Z} \alpha \, dx'' + \epsilon \beta_o \exp - \int_{Z_1}^{Z} \alpha \, dx'' + \int_{Z_1}^{Z} \beta \exp - \int_{x'}^{Z} \alpha \, dx'' \, dx'$$

where β is the blackbody function, we find that the terms which describe thermal emission from the earth and the gas are negligible at 2.3 μm, while the reflected sunshine term is unimportant at 4.6 μm. Thus, the radiation received, at 2.3 μm depends mainly on the amount of gas present and only very slightly on atmospheric temperature, though the temperature dependence of α, while at 4.6 μm the radiation depends strongly on both the atmospheric and surface temperatures. Indeed, if $\epsilon = 1$ and the temperatures of the lowest layer of the atmosphere and of the surface are the same, then the contribution to $I(4.6)$ from that layer is independent of α and the gas in this layer is "invisible" at this wavelength. If $\epsilon < 1$ (as is usual) and the earth radiance varies from point to point, then observations at 4.6 μm are possible only if the temperature distributions are known well enough to solve (1) or if the ground chopping technique is used.

The 2.3 μm region is free of thermal problems but shows strong interferences from other gases, mainly methane and water vapor, as shown on Figure 18, adapted from the Connes Planetary Atlas [3]. However, even though most of the CO lines are not easily distinguished on a conventional spectrum, such as in Figure 18, they still help to determine the number of photons received at these wavelengths and, thus, can be measured if the effects of the interferents can be accounted for. This can be done by the Barringer correlation interferometer which is being used on the COPE program.

The interferometer (described in more detail in the following section) forms the Fourier cosine transform of the received radiation. Since this is a linear operation, the transform (interferogram) contains the same information about the absorbing gases as does the spectrum but is displayed along a time rather than a frequency axis. Thus, just as the spectrum is a combination of distinctive lines, the interferogram is made up of distinctive signatures for each gas present (Fig. 19). The correlation technique depends on the fact that each point in the interferogram depends, in its own unique way, on the amounts of absorbers present. Thus, if the number of points M at which the interferogram J is measured equals or exceeds the number n absorbers present, it is possible to solve M equations for the n unknown amounts of gas present. This implies that it is possible to find a set of M numbers (a correlation of weighting function, W) such that

$$\sum_m \mathbf{J} \cdot \mathbf{W} = 0$$

if no CO is present and

$$\sum_m J \cdot W = (\text{amount of CO})$$

A breadboard model of the correlation interferometer, built under the COPE program, has demonstrated the measurement of less than 0.02 atm-cm CO in the presence of atmospheric amounts of CH_4 and H_2O. This would correspond to a change of 10 percent in the amount of CO in a round trip vertical path through an unpolluted atmosphere.

The interferogram also contains information on the amounts of methane and water present; these can be obtained from the same measurement by using a different correlation function, W .

This has also been done with the COPE breadboard, where applications of a suitable function W to the data where methane was an interferent in the CO measurement, yielded measurements of methane with better than 10 percent accuracy.

Correlation Interferometry

Correlation interferometry, like correlation spectrometry, is based upon cross-correlation of incoming signal against a stored replica. In this instance we work with interferograms which are the Fourier transforms of the input spectra [4, 5]. A basic Michelson correlation interferometer is shown in Figure 20. The beamsplitter B provides amplitude division of the input spectra from F which suffers reflections from mirrors M_1 and M_2 to recombine at the detector D . Here C is the compensator plate added by Michelson to balance the two optical arms. By suitable selection of position of movable mirror M_2 , the two beams can be caused to recombine at D in-phase and hence a minima occurs at B . If the compensator plate is now oscillated about its central position, a cyclic delay is introduced into the one arm, thereby unbalancing the interferometer to generate the well-known interferogram. Figure 20 shows the interferogram resulting from a single wavelength input. Figure 19 depicts the forms of various interferograms resulting from several spectral inputs, namely, a single discrete wavelength, two discrete wavelengths, and finally a series of equispaced spectral lines.

Recent progress in correlation interferometry has resulted in the development of the COPE field widened scanning Michelson correlation interferometer for General Electric's NASA-LRC COPE program. Figure 16 shows the first overtone absorption spectrum of CO in the 2.3 μm region, and Figure 21 shows its interferogram while Figure 22 shows a block diagram of the general signal processing involved. The interferogram centered on the delay region characteristic of CO is scanned by the oscillating refractor plate. The interferogram is heterodyned down to remove the high frequency interferogram carrier by mixing with a reference signal. The heterodyned signal is sampled and A to D converted for final processing within a minicomputer. At this final stage correlation functions are applied to reduce the effects of spectral interferences which, of course, show up as interferogram interferences in the delay domain of the interferometer. The process of correlation can best be visualized as the application of fixed amplitude digits cross-multiplied with the interferometer's output interferogram to normalize its output to represent zero CO gas output when no CO is present within the field of view, regardless of any interfering gases.

Theoretical modeling and atmospheric radiative transfer studies enable the weighting functions to be calculated for various model atmospheres. Subsequently, the instrument can have its in-program weights continually updated through actual field measurements to ensure no-gas output for no-gas input. In our particular COPE breadboard model, the interferogram is A to D converted and the weights held within the minicomputer as digital numbers applied to the digitized interferogram.

The advantages afforded by interferometers result from their large throughput, the spectral multiplex advantage, compact yet flexible design possibilities, and ready means for incorporation of correlative techniques for electronic processing, the latter obviating one of the major disadvantages of Fourier transform spectrometers, namely, that of transforming the Fourier output back to its original spectral form for analytical interpretation.

The COPE breadboard has the following salient features.

Aperture Interferometer	6.6 cm diameter
Telescope	22.0 cm diameter
Spectral Pass Bands	4240-4340 cm^{-1} and 2000-2200 cm^{-1}
Delay Scan Range	2.5 to 4.0 mm
No. of Sample Points	0 to 64
Sample Length	1 to 63 fringes
Scan Rate	1 Hz
No. of Scans Accumulated	1 to 500
NEP	1.6×10^{-11} $W/Hz^{1/2}$
Noise Equivalent Amount of CO (3 percent albedo and τ = 1 sec)	0.004 atm-cm

Conclusion

Problems of monitoring global air pollution from space platforms have been reviewed and experimental results presented of progress in the application of correlation techniques from the ultraviolet to the infrared. While results to date have been most encouraging, there is obviously considerable work to be done before a viable satellite air pollution monitoring system becomes a reality. Severe problems remain to be solved, particularly in the thermal infrared, but the technology is moving ahead rapidly, and there appears to be no insurmountable obstacle to the global mapping of most atmospheric pollutants from orbital altitudes.

References

1. Barringer Research Ltd.: Absorption Spectrometer Balloon Flight and Iodine Investigation. Final Report to NASA MSC Houston Texas Contract No. NAS9-9492, August 1970.

2. Stern, A. C.: Air Pollution. Academic Press, Second Edition, vol. 3, 1968.

3. Connes, J., et al.: Atlas des spectres infrarouges de Venns, Mars, Jupiter, et al. Saturne. Ed. du CNRS, Paris, 1969.

4. Barringer, A. R. and McNeill, J. D.: Advances in Correlation Techniques Applied to Spectroscopy. National Analysis Instrumentation Division of ISA Symposia, New Orleans, La., May 1969.

5. Dick, R. and Levy, G.: Correlation Interferometry. 1970 Aspen International Conference on Fourier Spectroscopy, AFCRL 71-0019, January 1971.

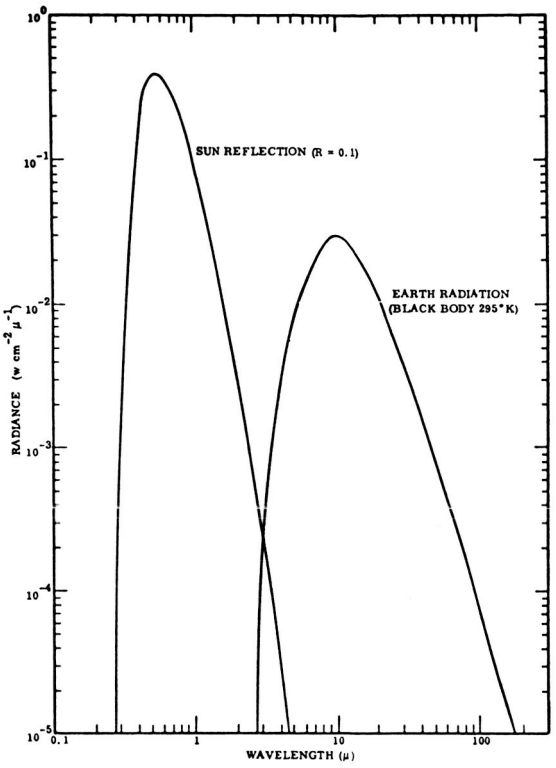

Figure 1. Contributions of the sun and earth to earth radiance.

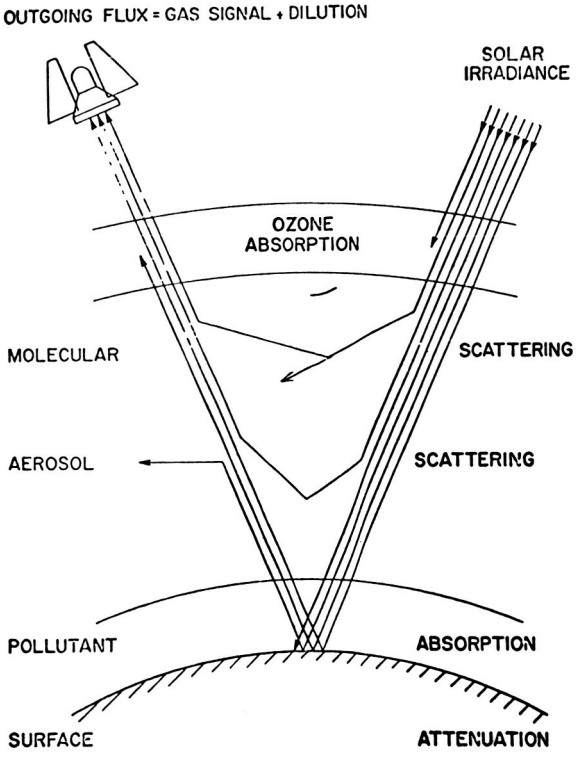

Figure 2. Attenuation and dilution in the ultraviolet.

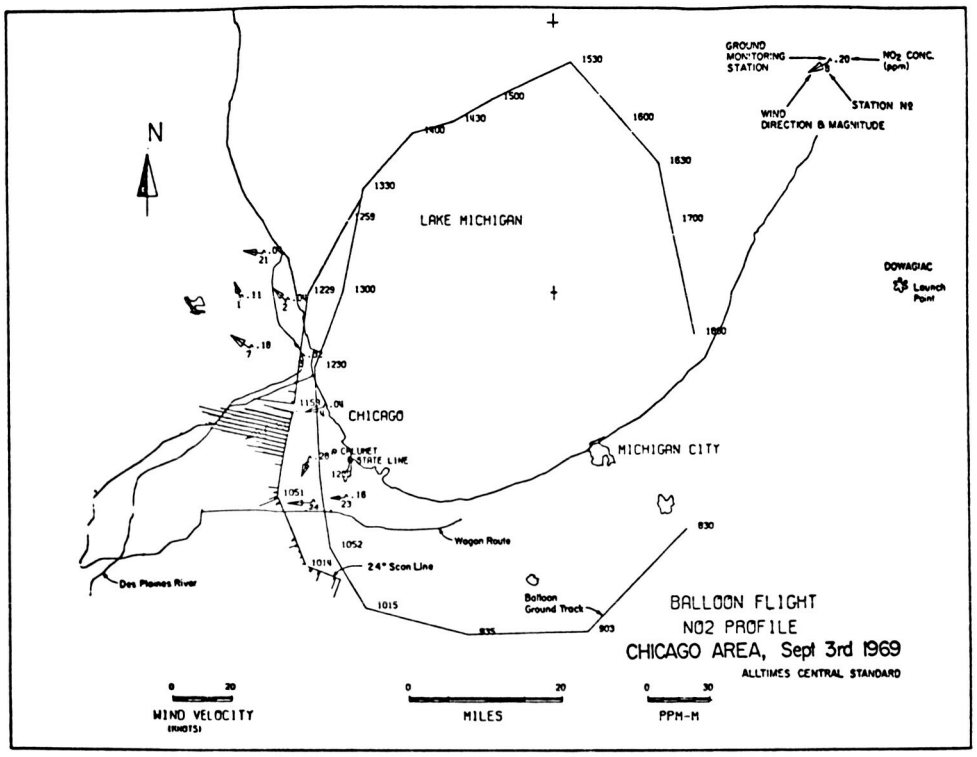

Figure 3. Computerized plot of the SO_2 spectrometer output signals.

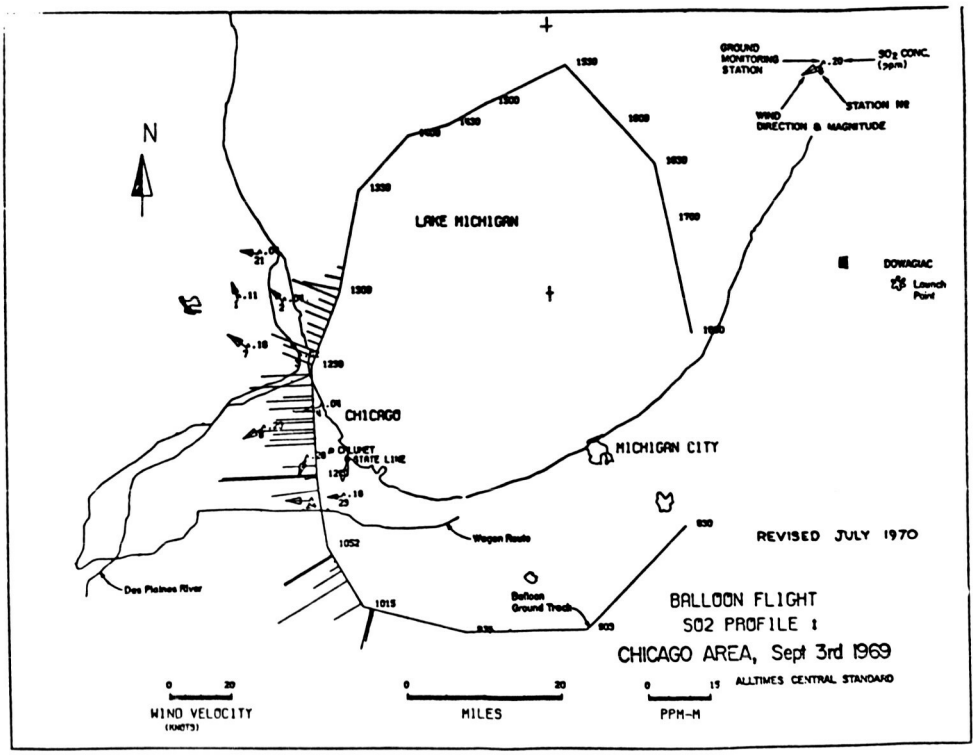

Figure 4. Vertical viewing direction.

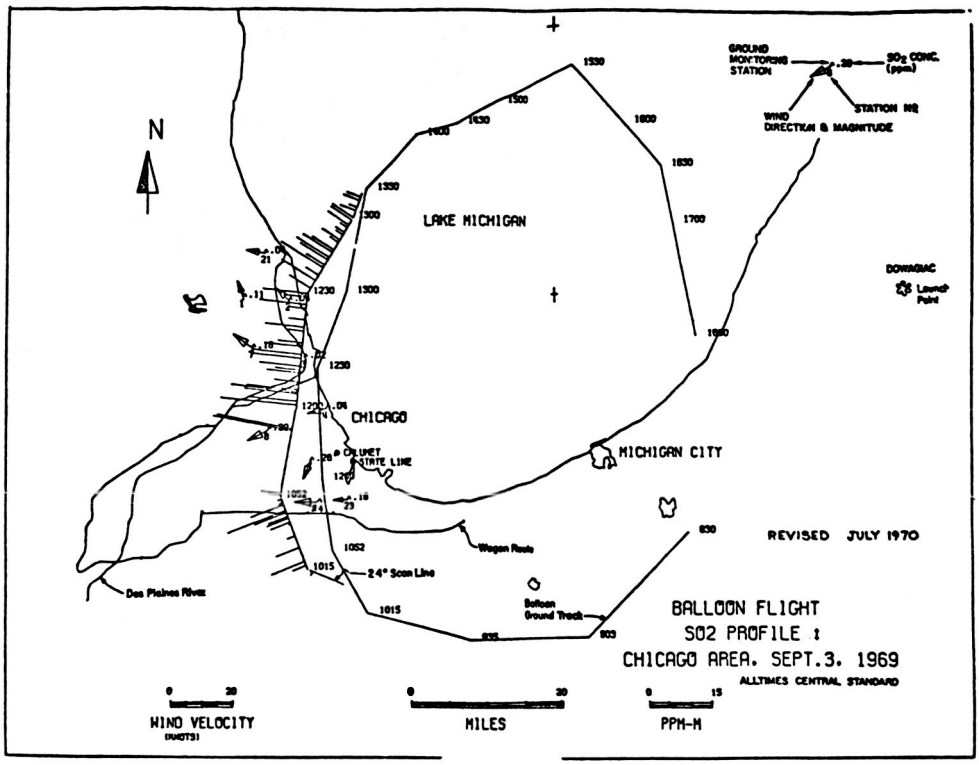

Figure 5. NO_2 data for 24 deg case.

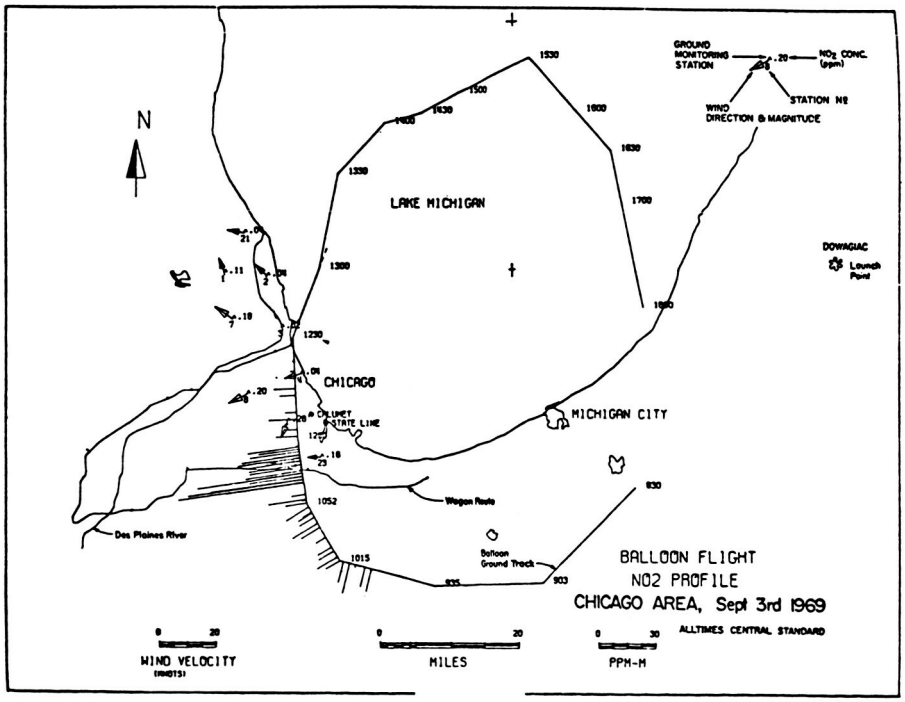

Figure 6. NO_2 data for ground vertical case.

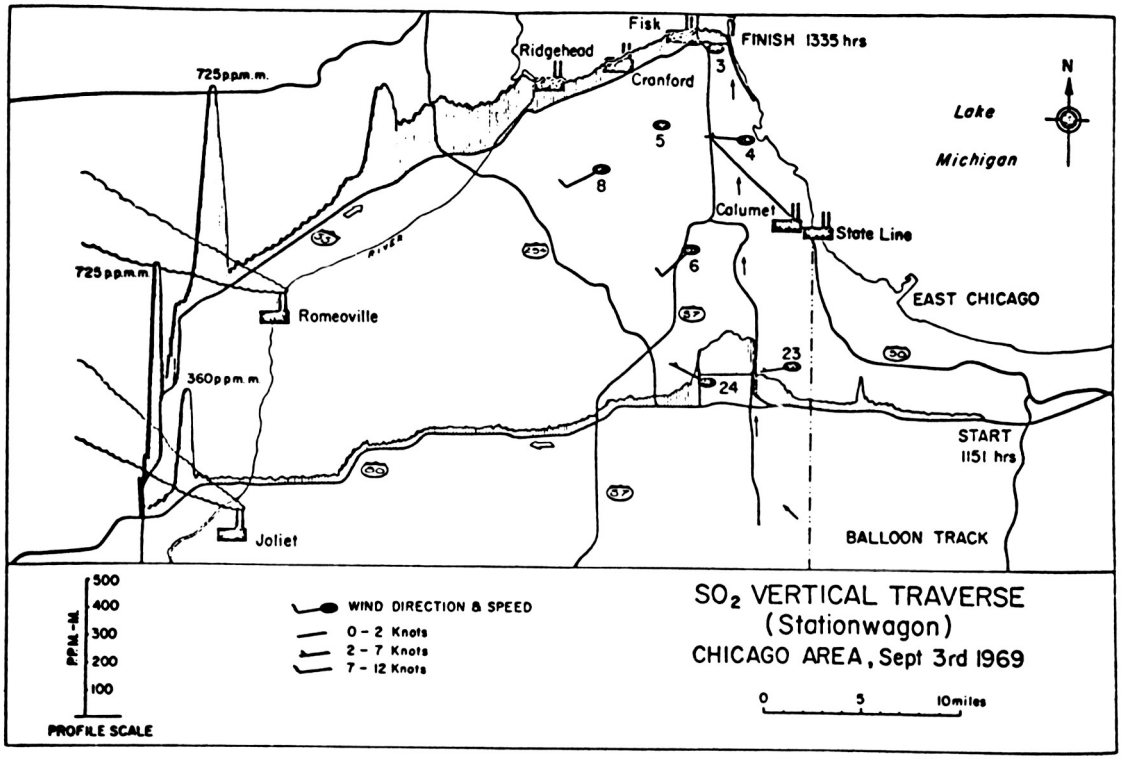

Figure 7. SO_2 vertical traverse.

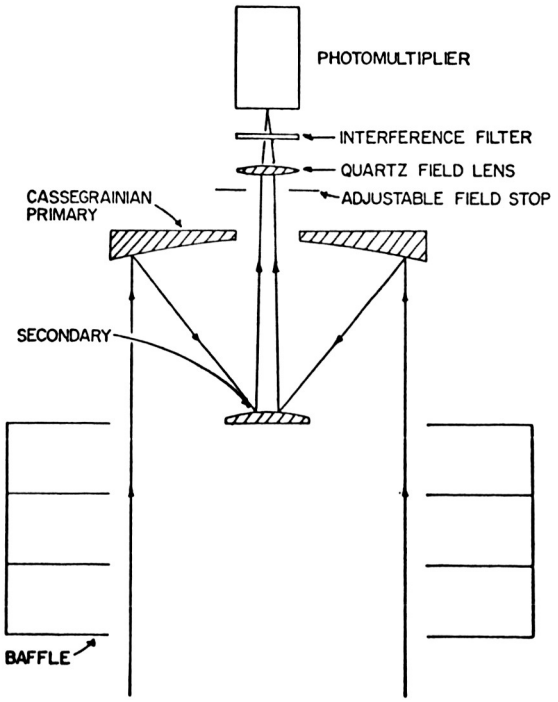

Figure 8. Ground chopper optics.

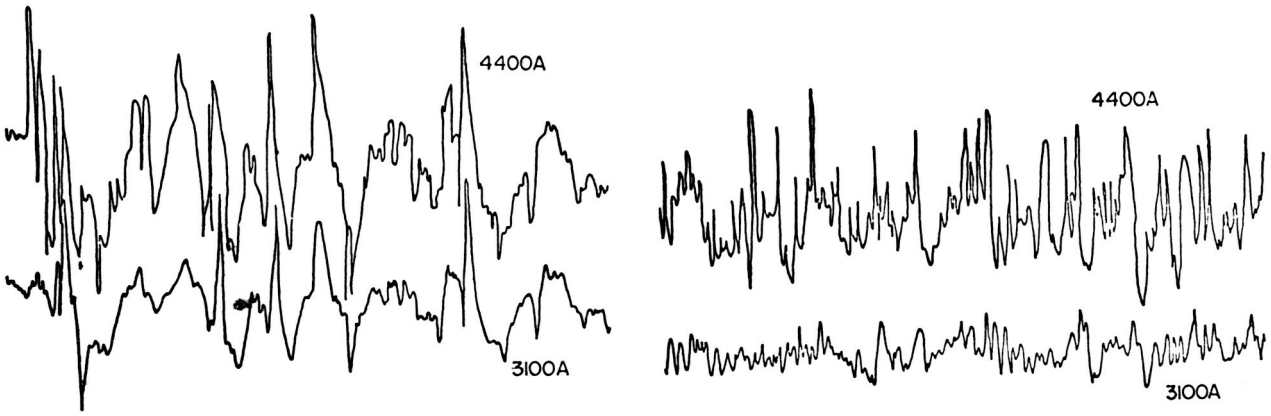

Figure 9. Ground chopped signal over Yellowknife (left) and natural terrain (right).

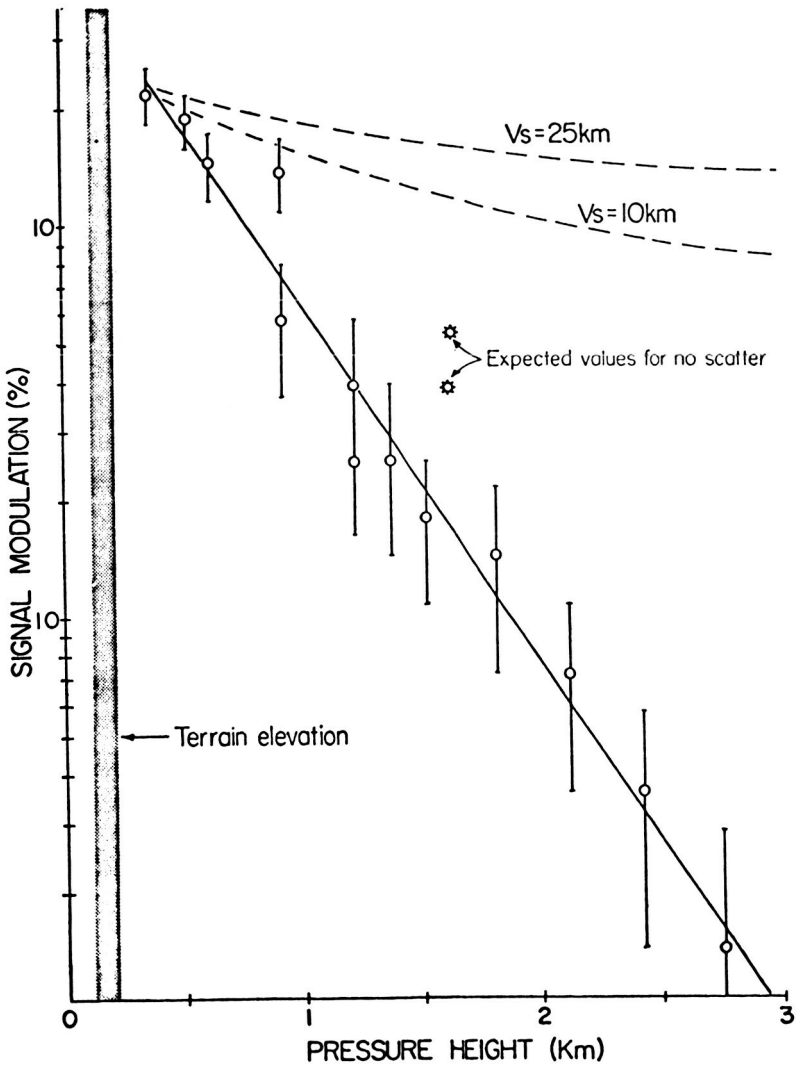

Figure 10. 3100 Å modulation versus height.

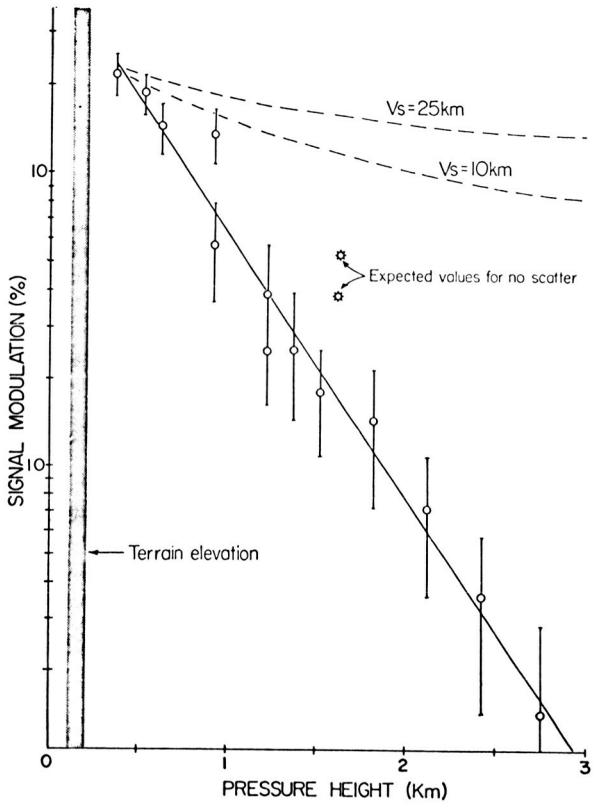

Figure 11. 3100 Å modulation versus height.

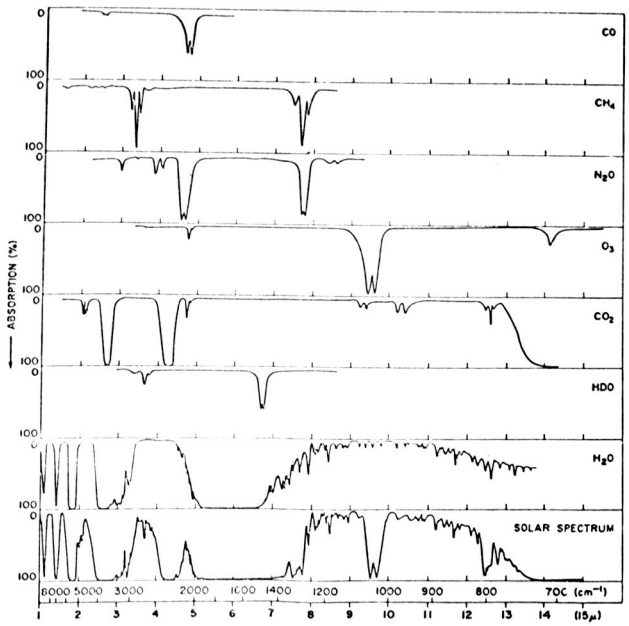

Figure 12. Comparison of the near-infrared solar spectrum with laboratory spectra of various atmospheric gases.[1]

1. Handbook of Geophysics and Space Environments. Air Force Cambridge Research Laboratories.

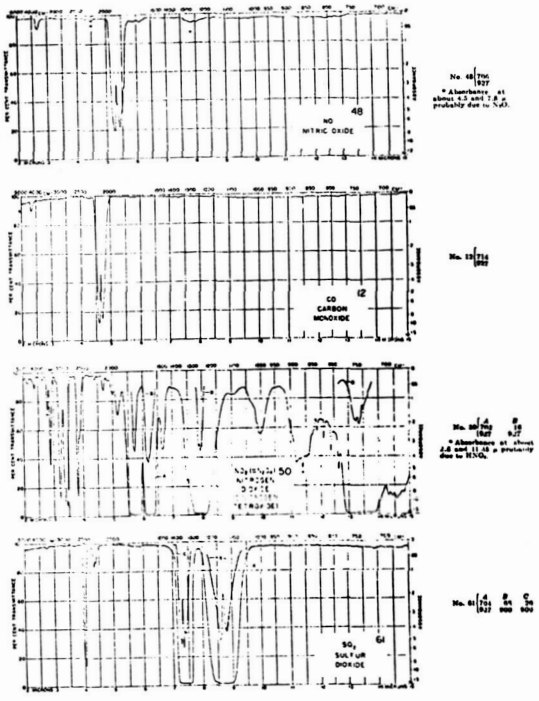

Figure 13. Absorption spectra for important atmospheric pollutants.[2]

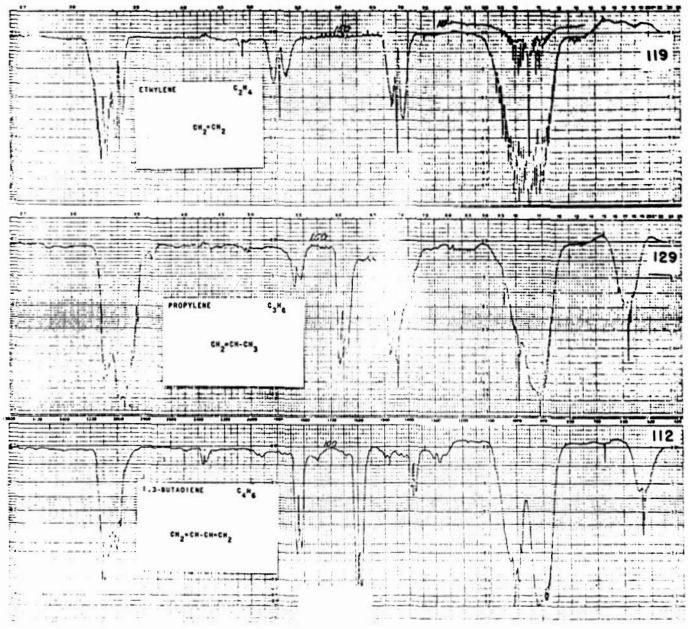

Figure 14. Spectra of three hypocarbons.[3]

2. Catalog of Infrared Spectra for Qualitative Analysis of Gases. Beckman Reprint R-93.

3. Infrared Spectra of Gases and Vapors. Vol. II, Grating Spectra by D. S. Earley and B. H. Blake, The Dow Chemical Company.

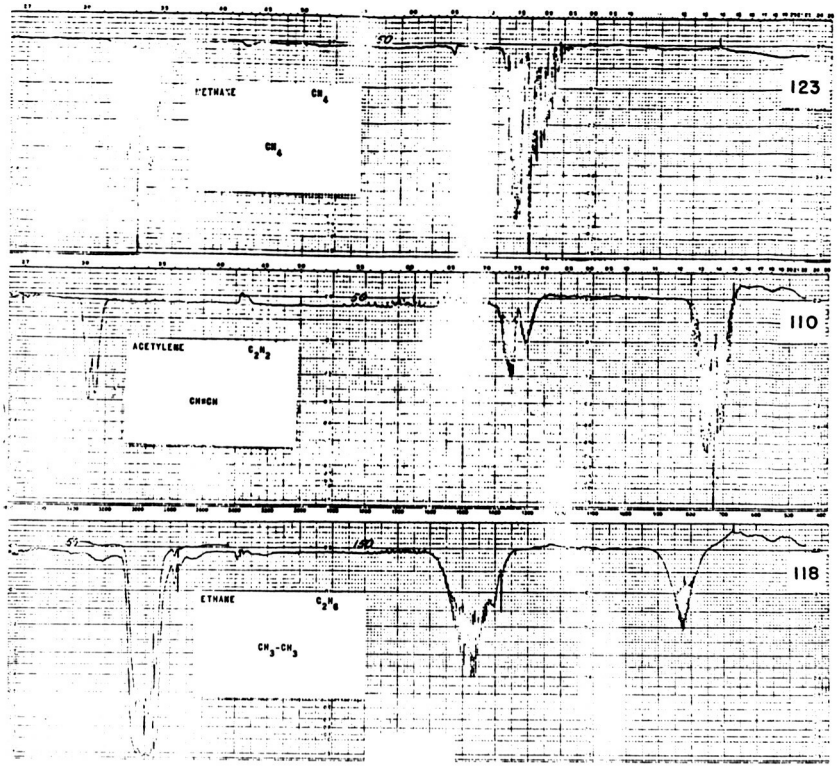

Figure 15. Spectra of three hypocarbons.[4]

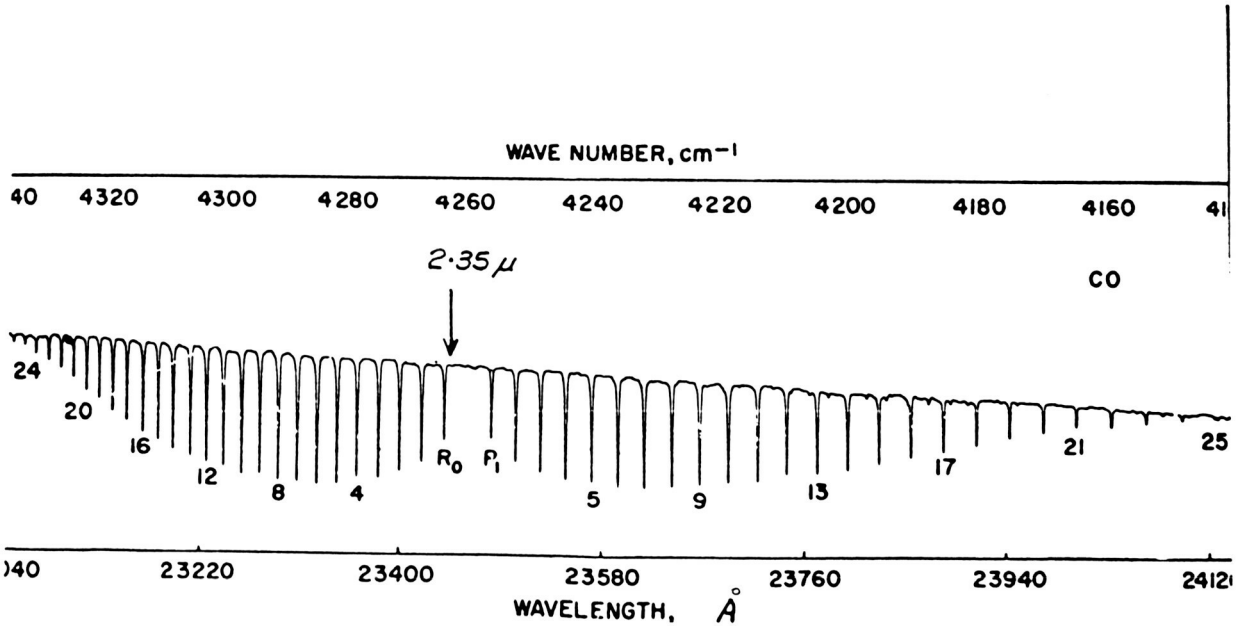

Figure 16. The 2-0 band of CO recorded with a 15 000 lines per inch grating with 20-cm pressure and 60-cm path (spectral slit about 0.15 cm^{-1}).

4. Ibid.

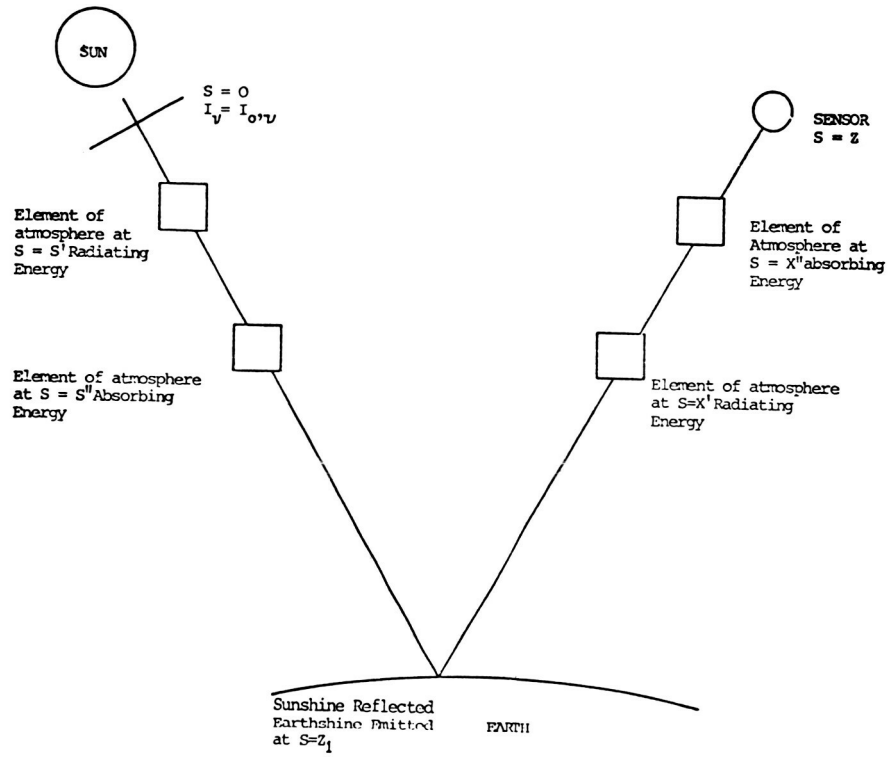

Figure 17. Geometry for mapping conditions.

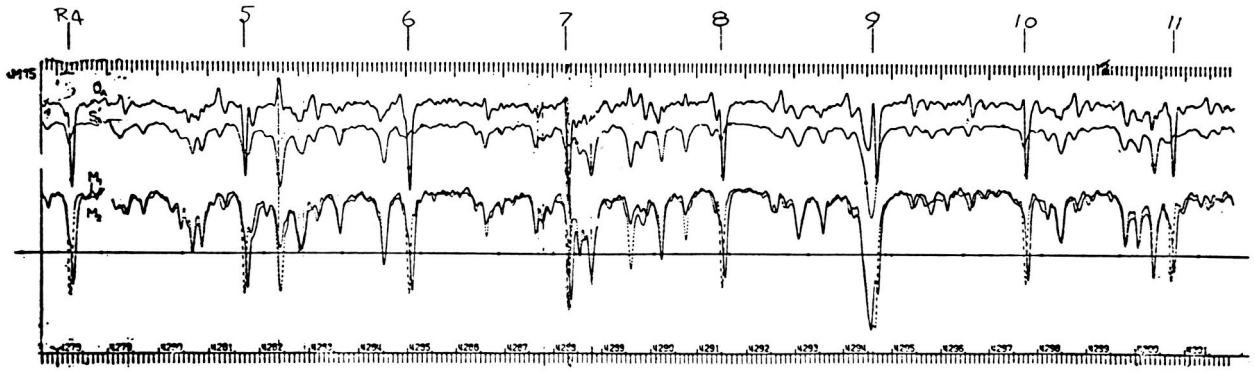

Figure 18. Solar spectrum showing 2-0 band of CO (S_A is the solar spectrum; the marks show the CO line positions).

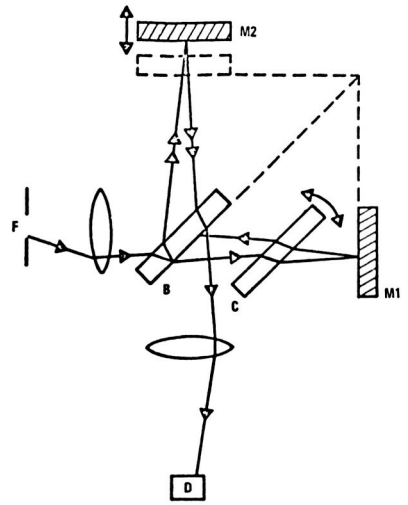

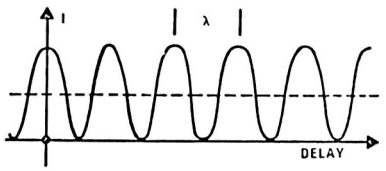

Figure 19. Fourier transforms.

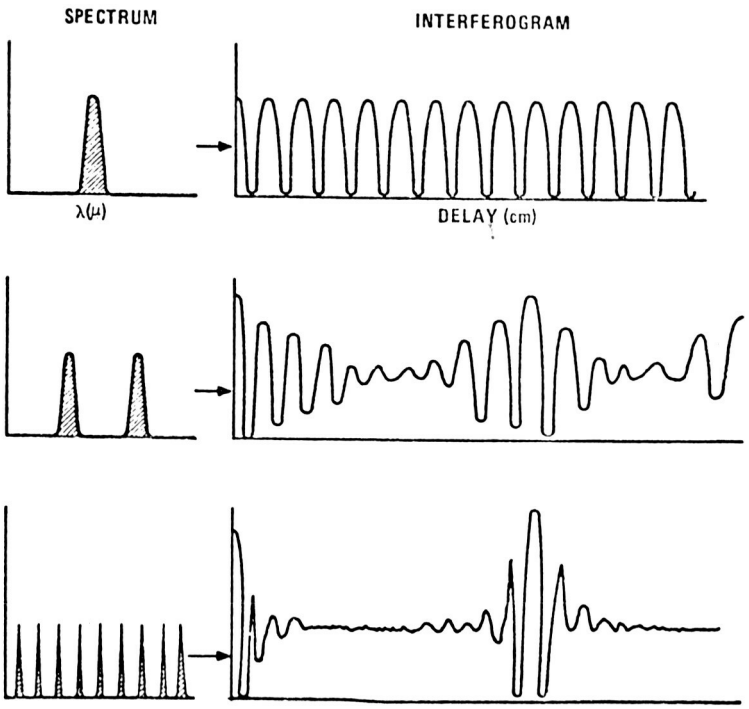

Figure 20. Correlation Michelson interferometer.

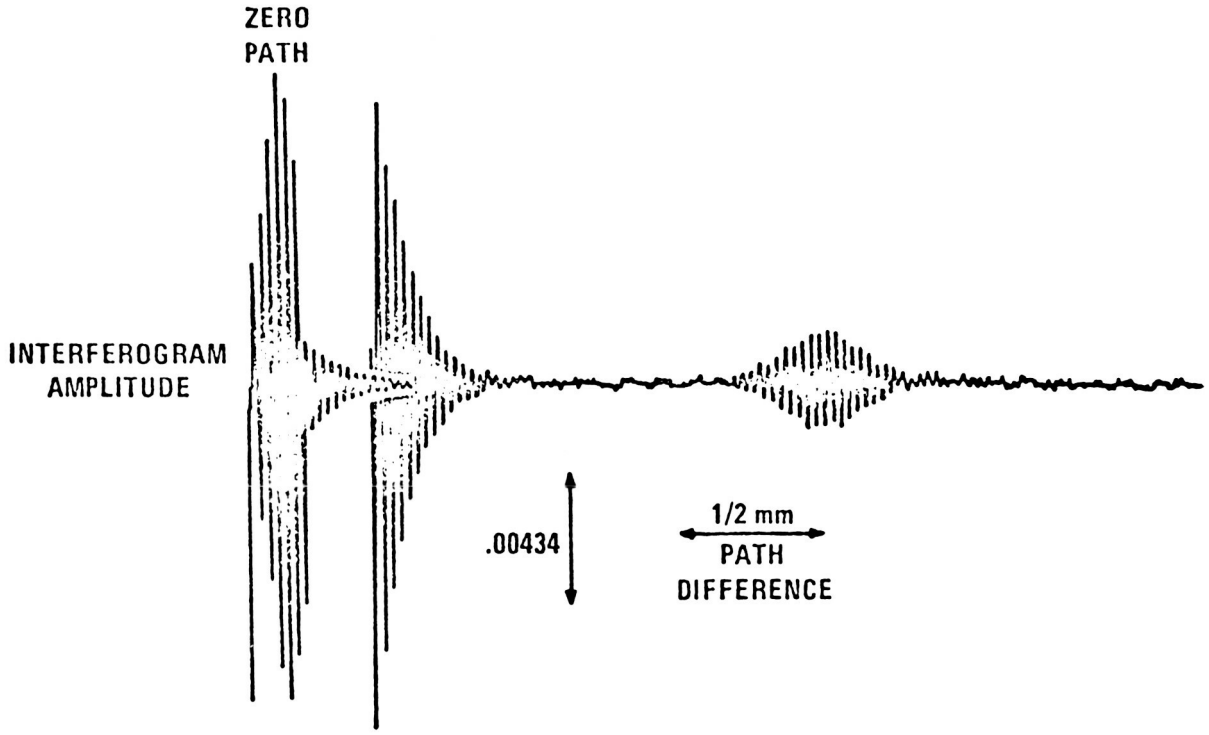

Figure 21. Interferogram.

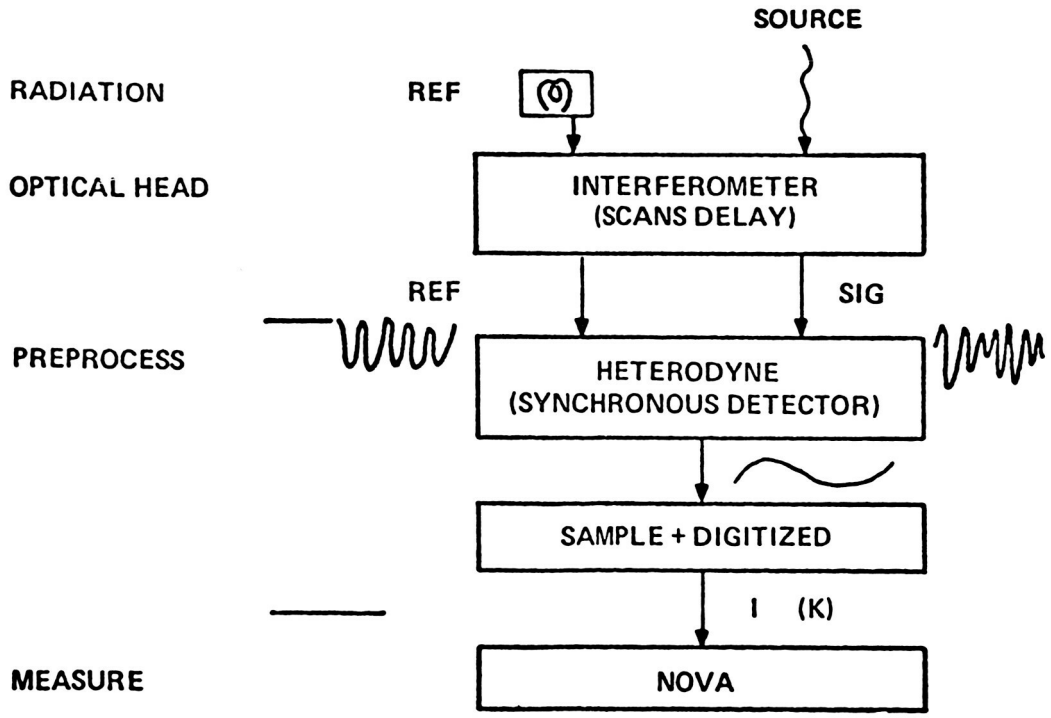

Figure 22. Interferometer system block diagram.